

# A simple classical model of infrared multiphoton dissociation

Ramakrishna Ramaswamy, Paul Siders, and R. A. Marcus

*A. A. Noyes Laboratory of Chemical Physics,<sup>a)</sup> California Institute of Technology, Pasadena, California 91125*  
(Received 14 April 1980; accepted 1 July 1980)

The classical mechanics of a system of two nonlinearly coupled oscillators driven by an oscillating electric field is studied. The presence of quasiperiodic and chaotic motion in the unforced system is shown to influence the nature of energy absorption. Two essentially different types of behavior are observed. In the first, energy is exchanged in a multiply periodic manner between the system and the forcing field. In the second regime, the energy exchange is erratic and a statistical analysis of a family of trajectories shows the role of the chaotic motion in the unforced system in the dissociation process. A theory for rate of photodissociation is presented and results are compared with those obtained from an ensemble of exact classical trajectories.

## I. INTRODUCTION

The phenomenon of multiphoton absorption in molecules has received considerable attention in the past few years.<sup>1,2</sup> The promise of isotope separation through selective absorption, and bond (or mode) specific chemistry in general, spurred experimental studies on several systems,<sup>2</sup> most notably SF<sub>6</sub>. Several theoretical models<sup>3,4</sup> have been proposed for the treatment of multiphoton absorption-induced dissociation. These include models with level population dynamics and use of an assumption of rapid intramolecular energy transfer process (which leads to an RRKM-type expression for the overall dissociation).<sup>3(a),(f)</sup> In some models<sup>3(a),(c)</sup> kinetic equations have been derived for the level population dynamics and that of the off-diagonal density matrix elements of such vibrationally excited molecules. One of the most prevalent (qualitative) schemes is based on the separation of molecular eigenstates into sets of discrete, quasicontinuous and continuous levels with coherent absorption in the discrete set and incoherent absorption by the quasicontinuum and continuum (e.g., Ref. 1), followed by dissociation from the continuum.

Due to the high densities of states at most energies in a typical molecule, any but the most simplified quantum treatments are presently impractical. A classical study, on the other hand, does not suffer from such a limitation (although all quantum effects cannot always be successfully incorporated). Of interest here is the actual classical phenomenology of (forced) driven molecular systems, and in particular the nature of mode-mode energy transfer in facilitating dissociation.

As an initial approach to this question, we study a system of nonlinearly coupled oscillators under the influence of an external field coupled to only one of the degrees of freedom. In essence, this resembles a simplified molecule interacting with a laser field. Forced oscillators have often been studied in the literature in the context of laser-molecular interaction,<sup>5</sup> and also in

the theory of mechanical vibrations.<sup>6</sup> (The single forced oscillator has an extensive history,<sup>7</sup> as in the Duffing equation.) For systems with more than one vibrational degree of freedom, exact analytic results are usually not possible when the coupling is nonlinear, even in the autonomous case. For the latter case, there is the well-known KAM theorem<sup>8(a),8(b)</sup> regarding the stability of the motion in nonlinear, nonintegrable Hamiltonian systems. An extension of this theorem<sup>8(c)</sup> is applicable to the nonautonomous case at hand and guarantees the stability of the (driven) motion for sufficiently small forcing fields.

In Secs. II and III are described the classical Hamiltonian and some features of the autonomous and forced system dynamics. Analytical and statistical descriptions are presented in Sec. IV, followed by numerical results from trajectories and comparison with the theory of Sec. IV in Sec. V. A concluding discussion is given in Sec. VI.

## II. THE CLASSICAL HAMILTONIAN OF THE AUTONOMOUS SYSTEM

The Hamiltonian of the unforced coupled oscillator system investigated here is

$$H' = \frac{1}{2}(p_x^2 + p_y^2 + \omega_x^2 x^2 + \omega_y^2 y^2) + \lambda x(y^2 + \eta x^2), \quad (2.1)$$

where  $(x, p_x, \omega_x)$  and  $(y, p_y, \omega_y)$  denote the coordinate, momentum, and zeroth-order frequency, respectively. The values of parameters chosen here are  $\omega_x = 1.3$ ,  $\omega_y = 0.7$ ,  $\lambda = 0.1$ , and  $\eta = -1$ ; this type of Hamiltonian has often been used in the nonlinear dynamics literature.<sup>9</sup> The three saddle points for the dissociation channels are located at  $(x, y) = (5.633, 0)$  and  $(-2.45, \pm 7.708)$  with a minimum dissociation energy of  $E = 6.54$  units (at the last two points).

It is well known that the dynamics of the Hamiltonian  $H$  has a rich structure associated with it,<sup>9(a)</sup> manifested as trajectories that are either quasiperiodic in time or "chaotic." The essential difference between these two types of motion is that the former trajectories are confined to a torus in phase space while the latter are not.

<sup>a)</sup>Contribution Number 6210.

This difference is easily characterized by the Poincaré surface of section,<sup>9</sup> which for the former type are smooth curves, while for the latter they are a seemingly random splatter of points.

It has become convenient in the discussion of such systems to describe a "critical energy"  $E_c$  above which the initial conditions lead to mainly chaotic-type trajectories.<sup>10</sup> (It must be pointed out that either type of behavior can occur at any energy. Only the relative fraction of chaotic trajectories changes with energy.) For purposes of characterization, the surface of section for  $x=0$  and  $p_x>0$  at selected energies is shown in Fig. 1. The areas of stability (i.e., leading to quasiperiodic motion) persist up to high energies and are primarily located along the positive diagonal in the  $(y, p_y)$  plane. We can further extract the relative fractions of phase space that lead to chaotic motion by measuring the relative areas not covered by the smooth curves in Fig. 1 as in Fig. 2.

The ground state energy of the quantized system can

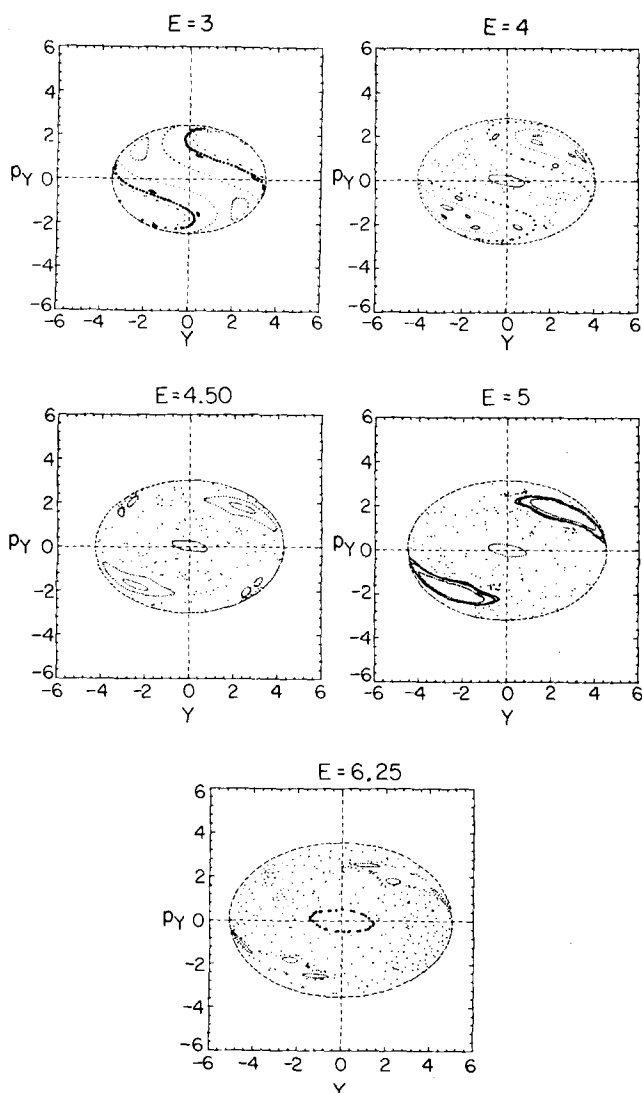


FIG. 1. Surfaces of section for the present system at selected energies.

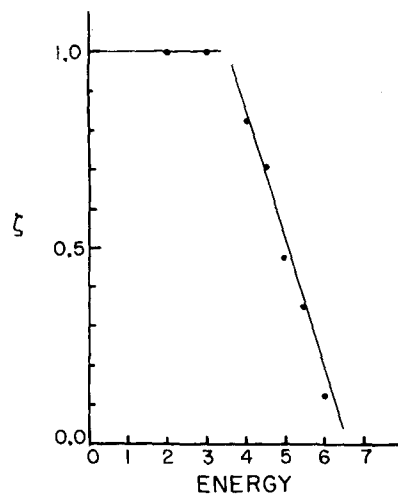


FIG. 2. Relative fraction of phase space covered by tori as a function of energy.

be determined semiclassically by a variety of methods.<sup>9(b),11</sup> We find the semiclassical zero-point energy to be<sup>11(c)</sup> 0.9970, which is also the exact quantum result.<sup>12</sup>

### III. THE NONAUTONOMOUS (FORCED) SYSTEM

The interaction with the driving term is chosen to occur through the  $y$  degree of freedom, giving the total Hamiltonian

$$H = H' - Fy \cos \omega t. \quad (3.1)$$

Hamilton's equations obtained from Eq. (3.1) are

$$\begin{aligned} \dot{x} &= p_x, & \dot{y} &= p_y, \\ \dot{p}_x &= -(\omega_x^2 x + \lambda y^2 + 3\lambda \eta x^2), \\ \dot{p}_y &= -(\omega_y^2 y + 2\lambda xy) + F \cos \omega t, \end{aligned} \quad (3.2)$$

and can be integrated numerically<sup>13</sup>; the initial conditions uniquely determine the trajectory in phase space.

We first consider some principal qualitative features associated with a typical such trajectory. Shown in Fig. 3 is the total energy content of the oscillators  $E$  [i.e.,

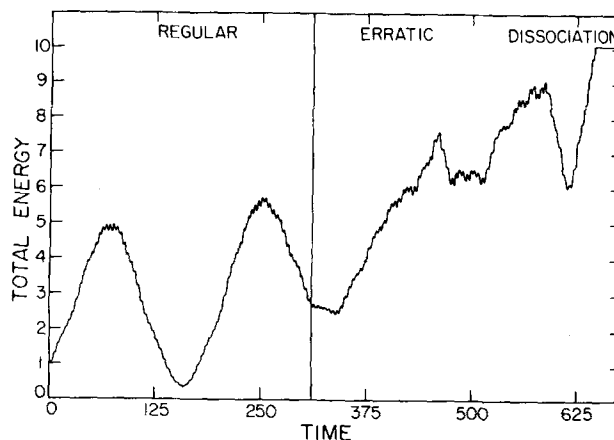


FIG. 3. Time dependence of the total energy for a given set of initial conditions ( $x=0.2284$ ,  $y=1.2776$ ,  $p_x=-0.2115$ ,  $p_y=0.9945$ ,  $F=0.1$ ), in rounded-off values. The separate regimes are classified as periodic and erratic.

$H'(t)$ ] as a function of time. Two regions of behavior may be identified, separated by a vertical line in Fig. 3:

(1) *regular* energy exchange between the system and the field, with a definite set of associated frequencies;

(2) *erratic* energy exchange between the system and the field with several associated frequencies—in marked contrast to the previous region. Arrival at this region was, for all trajectories studied here, ultimately accompanied by dissociation, as in Fig. 3.

A related type of behavior was observed in an earlier classical trajectory study<sup>5(b)</sup> of multiphoton absorption in CD<sub>3</sub>Cl [Fig. 4 of Ref. 5(b)]: The presence of nine normal modes of vibration in CD<sub>3</sub>Cl made the motion more complicated than that in Fig. 3. Nevertheless, in that study there seems to be rather periodic energy exchange between the molecule and the field in the initial period of excitation, followed by energy absorption with somewhat erratic oscillations, similar qualitatively to the present observations. The actual behavior of individual trajectories can differ considerably in the extents to which they sample the two regimes. [See also Fig. 2 of Ref. 5(d).] It was noted in the CD<sub>3</sub>Cl + laser system that different initial conditions led to widely different dissociation times—an observation that is common to this work. Before presenting the numerical results obtained by integrating Eqs. (3.2), we first give an approximate analytic and statistical theory of the process.

#### IV. ANALYTICAL AND STATISTICAL DESCRIPTIONS

##### A. The regular regime

We first examine the regular regime. The first analysis given below is based on the Krylov–Bogoliubov–Mitropolsky (KBM) method,<sup>14</sup> which has the advantage of physical intuitiveness; the perturbation solution is constructed upon an approximate solution.

##### 1. Application of KBM-type theory

It is convenient to combine Eqs. (3.2) to yield

$$\ddot{x} + (\omega_x^2 + 3\lambda\eta x)x + \lambda y^2 = 0, \quad (4.1a)$$

$$\ddot{y} + (\omega_y^2 + 2\lambda x)y = F \cos \omega t. \quad (4.1b)$$

The case of principal interest here is one permitting extensive energy absorption—that of zeroth-order *external* resonance, i. e.,  $\omega = \omega_y$ . Exact solutions to Eqs. (4.1) with  $\lambda = 0$  are divergent (secular, i. e., they grow linearly in time) for  $\omega = \omega_y$ . In practice, the nonlinearity (the  $\lambda xy^2$  term) removes the secularity. Equation (4.1) is rewritten in terms of a perturbation parameter  $\lambda$  to facilitate the application of KBM:

$$\ddot{x} + \omega_x^2 x = \lambda f_x(x, y) + \lambda F_x \cos \omega t, \quad (4.2a)$$

$$\ddot{y} + \omega_y^2 y = \lambda f_y(x, y) + \lambda F_y \cos \omega t, \quad (4.2b)$$

with

$$F_x \equiv 0, \quad F_y = F/\lambda, \quad f_x = -(y^2 + 3\eta x^2), \quad f_y = -2xy. \quad (4.2c)$$

The solution to Eqs. (4.2) with  $\lambda = 0$  is immediately seen to be

$$x(t) = A_x \cos(\omega_x t + \theta_x), \quad y(t) = A_y \cos(\omega_y t + \theta_y). \quad (4.3)$$

We seek the  $\lambda \neq 0$  solution by introducing time-dependent amplitudes  $A_\alpha(t)$  and  $A_y(t)$  and phases  $\theta_\alpha(t)$  and  $\theta_y(t)$ , with the standard additional restriction of KBM,<sup>14</sup> i. e., with

$$\begin{aligned} \dot{x}(t) &= -\omega_x A_x \sin(\omega_x t + \theta_x), \\ \dot{y}(t) &= -\omega_y A_y \sin(\omega_y t + \theta_y). \end{aligned} \quad (4.4)$$

It is straightforward to expand  $A_\alpha(t)$  and  $\theta_\alpha(t)$ ,  $\alpha \equiv x, y$ , in powers of  $\lambda$ :

$$\begin{aligned} A_\alpha(t) &= a_\alpha(t) + \lambda \tilde{F}(A_x, A_y, \theta_x, \theta_y) + \dots, \\ \theta_\alpha(t) &= \psi_\alpha(t) + \lambda \tilde{G}(A_x, A_y, \theta_x, \theta_y) + \dots, \end{aligned}$$

where  $a$ ,  $\psi$ ,  $\tilde{F}$ , and  $\tilde{G}$  are to be determined. In the first approximation, to which we restrict our attention here, the  $\tilde{F}$ 's and  $\tilde{G}$ 's, which are related to the fast variables of the problem, are ignored, and one obtains<sup>6</sup>

$$\begin{aligned} \dot{a}_x &= 0, \quad a_x \dot{\psi}_x = \lambda a_x^2 / 4\omega_x, \\ \dot{a}_y &= -\lambda F_y \sin \psi_y / 2\omega_y, \\ a_y \dot{\psi}_y &= -\lambda (F_y \cos \psi_y - a_x a_y) / 2\omega_y. \end{aligned} \quad (4.5)$$

Solving Eqs. (4.5), one finds

$$\begin{aligned} a_x &= \text{const.} = A_x^0, \quad a_y = A_y^0 \cos \psi_y, \\ \psi_x &= \gamma + \delta t, \quad \psi_y = \alpha + \beta t, \end{aligned} \quad (4.6)$$

where  $\alpha$  and  $\gamma$  are the initial phases, and

$$\beta = \lambda A_x^0 / 4\omega_y, \quad \delta = \lambda F_y^2 / 2\omega_x (A_x^0)^3, \quad A_y^0 = 2F_y / A_x^0. \quad (4.7)$$

The results in this quasiperiodic regime are given later in Fig. 4(a).

##### 2. Application of Lie transforms

A more elegant approach to the perturbative solution in the regular regime can be effected through the method of Lie transforms.<sup>15</sup> A canonical transformation from the variables  $(\mathbf{q}, \mathbf{p})$  ( $q_1 \equiv x$ ,  $q_2 \equiv y$ ,  $p_1 \equiv p_x$ ,  $p_2 \equiv p_y$ ) to new variables  $(\xi, \eta)$  is defined through a Lie generator.

$$\begin{aligned} S &= S(\xi, \eta; \lambda) \\ &= S_1(\xi, \eta) + \lambda S_2(\xi, \eta) + \dots \end{aligned} \quad (4.8)$$

by the relations

$$\begin{aligned} q_i &= \xi_i + \sum_{n=1}^{\infty} \frac{\lambda^n}{n!} D_s^{n-1} \frac{\partial S}{\partial \eta_i} \equiv e^{\lambda D_s} \xi_i, \\ p_i &= \eta_i - \sum_{n=1}^{\infty} \frac{\lambda^n}{n!} D_s^{n-1} \frac{\partial S}{\partial \xi_i} \equiv e^{\lambda D_s} \eta_i, \end{aligned} \quad (4.9)$$

where the operator  $D_s$  is the Lie (Poisson) bracket

$$\begin{aligned} D_s^0 f &= f, \\ D_s^1 f &= \sum_k \left( \frac{\partial f}{\partial \xi_k} \frac{\partial S}{\partial \eta_k} - \frac{\partial f}{\partial \eta_k} \frac{\partial S}{\partial \xi_k} \right), \end{aligned} \quad (4.10)$$

and

$$D_s^n f = D_s^1 (D_s^{n-1} f).$$

From Eqs. (4.9), any continuous function of  $(q, p)$  can

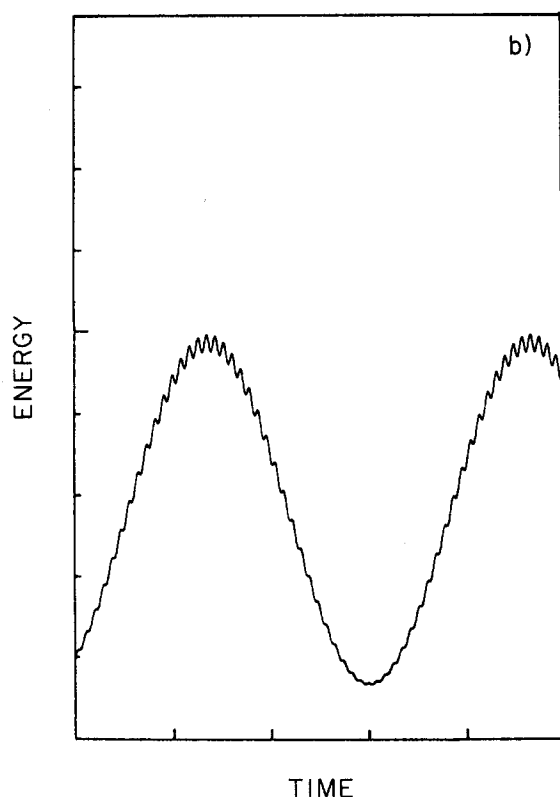
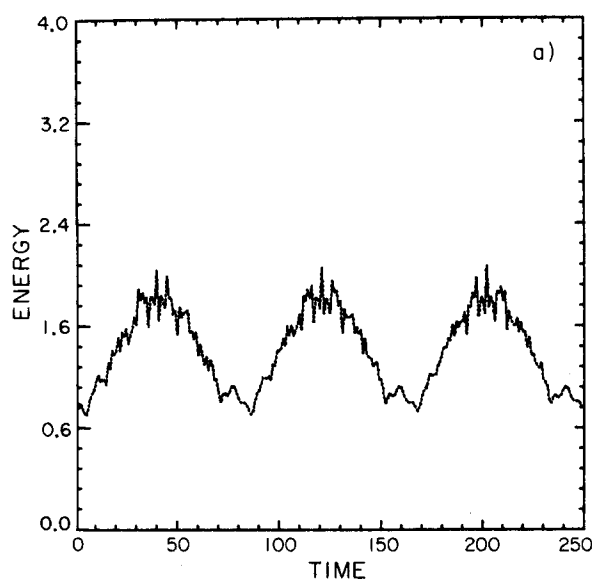


FIG. 4. (a) Total energy behavior in the regular regime predicted by the KBM-type analysis. (b) Total energy behavior in the regular regime predicted by the Lie-transform analysis (arbitrary units).

be transformed according to

$$f(q, p) = \sum_{n=0}^{\infty} \frac{\lambda^n}{n!} D_s^n f(\xi, \eta) \equiv e^{\lambda D_s} f(\xi, \eta). \quad (4.11)$$

The algorithm for determining the Lie generator  $S$  is well known.<sup>16</sup> We utilize the perturbation method including up to first order in  $\lambda$  terms to determine new

frequencies  $\tilde{\omega}_x$  and  $\tilde{\omega}_y$ , of motion in the  $x$  and  $y$  degree of freedom for the autonomous system defined in Eq. (2.1). (One could also have applied the method directly to the nonautonomous system, though now with one extra degree of freedom.<sup>16(b)</sup>)

For the system at hand, the Lie generator is given by [using the algorithm in Ref. 16(a)]<sup>16(c)</sup>

$$S = - \frac{\lambda}{4\omega_x^2\omega_y^2(\omega_x + 2\omega_y)} [\omega_y^2(3\omega_x + 4\omega_y)\eta_1\xi_2^2 + (\omega_x + 4\omega_y)\eta_1\eta_2^2 + 2\omega_x^2\omega_y\eta_2\xi_1\xi_2] + O(\lambda^2). \quad (4.12)$$

Thus, for the problem with  $F = 0$ , to order  $\lambda$ ,

$$\begin{aligned} x(t) &= \xi_1 + \frac{\partial S}{\partial \eta_1}, & p_x(t) &= \eta_1 - \frac{\partial S}{\partial \xi_1}, \\ y(t) &= \xi_2 + \frac{\partial S}{\partial \eta_2}, & p_y(t) &= \eta_2 - \frac{\partial S}{\partial \xi_2}, \end{aligned} \quad (4.13)$$

where

$$\begin{aligned} \xi_1 &= C_1 \cos(\tilde{\omega}_x t + C'_1), & \eta_1 &= -C_1 \omega_x \sin(\tilde{\omega}_x t + C'_1), \\ \xi_2 &= C_2 \cos(\tilde{\omega}_y t + C'_2), & \eta_2 &= -C_2 \omega_y \sin(\tilde{\omega}_y t + C'_2), \end{aligned} \quad (4.14)$$

and

$$\tilde{\omega}_y = \omega_y - \frac{\lambda(P_0)^{1/2}}{(2\omega_x\omega_y^2)^{1/2}} - \frac{\lambda^2[(5\omega_x + 8\omega_y)P_2 - 8P_0(\omega_x + 2\omega_y)]}{4\omega_x^2\omega_y^2(\omega_x + 2\omega_y)}, \quad (4.15)$$

with

$$P_0 = \left\{ \frac{1}{12} [-2(\omega_x - 2\omega_y)(2\omega_x\omega_y^2)^{1/2}/\lambda + \sqrt{(8(\omega_x - 2\omega_y)^2\omega_x\omega_y^2/\lambda^2 + 24P_2)}] \right\}^2$$

and

$$P_2 = \omega_x C_1^2 + \frac{\omega_y}{2} C_2^2, \quad C_1, C_2, C'_1, \text{ and } C'_2 \text{ are constants.}$$

In the regular regime, we find that the overall behavior of the total energy is roughly duplicated simply by treating the total system (with  $F \neq 0$ ) as a single,  $y$ -type oscillator of altered frequency  $\tilde{\omega}_y$ , driven by the external field with  $\tilde{\omega}_y$ , given by Eq. (4.15). Thus, we now get the equation of motion

$$\ddot{y} + \tilde{\omega}_y^2 y = F \cos \omega t, \quad (4.16)$$

where  $\tilde{\omega}_y$  is no longer equal to  $\omega_y$ . Equation (4.16) is easily solved to yield

$$y(t) = K \sin(\tilde{\omega}_y t + \theta_1) + \frac{F}{\tilde{\omega}_y^2 - \omega^2} \cos \omega t, \quad (4.17)$$

where  $K$  and  $\theta_1$  are determined by the initial conditions.

The total energy behavior, i. e.,  $H'(t)$ , determined by the above equations is shown in Fig. 4(b), and it is seen by comparison with Fig. 3 that the overall features have the same qualitative behavior as the numerical results in the regular regime. A quantitative comparison is given later. It may be noted that the variable corresponding to  $\beta$  in Eqs. (4.6) is given by the Lie-trans-

form method as  $\frac{1}{2}(\bar{\omega}_y - \omega)$  and determines the "long" periodicity in the energy behavior. The shorter oscillations are determined by  $\omega_y$ , with side bands related to  $\bar{\omega}_y - \omega$ .

## B. The erratic regime

In this regime, the total energy of the oscillators fluctuates in time in an irregular manner. The difference between this and the previous regime is similar to that between quasiperiodic and chaotic motion in the autonomous system. The current absence of rigorous analytic methods that are applicable for treatment of chaotic behavior makes a statistical approach a useful first alternative. The analysis is thus applicable to an ensemble of trajectories rather than any particular one. We shall make the following assumptions: (1) In the periodic regime for an individual trajectory, the total energy is approximately the same for all maxima. (2) The erratic regime sets in for an individual trajectory when the forcing term leads the system into a portion of phase space where the underlying motion is chaotic. (3) All systems in the erratic regime ultimately dissociate. (4) The probability of entering the erratic regime at a given peak is simply that fraction  $(1 - \zeta)$  of phase space *not* covered by tori.

With the above assumptions, we can deduce the following: (1) There is a time lag in the appearance of dissociation products which is related to the minimum time required to absorb the requisite energy  $(E_{\text{diss}} - E_0)$ , where  $E_0$  is the energy before the laser is started. The fraction of trajectories surviving beyond the first maximum is  $\zeta$ . At subsequent maxima, then, the fraction of surviving trajectories is  $\zeta^n$ , where  $n=1, 2, 3, \dots$  indexes the successive maxima. The long period of the  $y$  motion is  $2\pi/\beta$ , so that of  $E_y$  (the energy of the  $y$  degree of freedom) and of  $E$  is  $\pi/\beta$ . Measuring time from the first peak, we note that the time at the subsequent peaks has the values  $\pi/\beta, 2\pi/\beta, \dots$  [cf. Eq. (4.5)]. Thus, the fraction  $f_s(t)$  of trajectories that are surviving at time  $t$  is given by

$$f_s(t) = \zeta^{\beta t/\pi} \quad (4.18)$$

Here  $\beta$  depends on the properties of the regular regime, and  $\zeta$  is dependent on those of the autonomous dynamical system in the regular-chaotic regime.

Equations (4.6) and (4.18) embody the central results of the above simple theory of the dissociation process. In the following section, we present some numerical results for  $f_s(t)$  calculated from trajectories that can be directly compared to Eq. (4.18) and discuss the implications of the above analysis.

## V. NUMERICAL RESULTS.

### A. Regular regime

In the quasiperiodic regime, a quantum state has its analog in an "eigentorus." Accordingly, we analyze the forced system in terms of a family of trajectories whose initial conditions are chosen uniformly over this torus. The torus was in turn determined by the approximate method of Ref. 11(c).

From the simple KBM-type analysis of the regular regime in Sec. IVA, the periodic solution for  $y(t)$  is seen to be a product of two sinusoidal functions, with a "short" periodicity close to that of the uncoupled  $y$  oscillator and a "long" periodicity given by  $2\pi/\beta$ . By using Eqs. (4.6) or (4.17), the total energy behavior in the regular regime is qualitatively reproduced: For each, both the period and the amplitude of the long-period oscillation in the total energy (Fig. 3) in the regular regime agree to a factor of about 2 with the exact results.<sup>17</sup> [Because of the simplifying approximation<sup>16(c)</sup> regarding a resonant phase angle, Eqs. (4.6) and (4.17) do not allow for the appreciable  $x$  and  $y$  energy exchange occurring in the autonomous system.] Further calculations are planned.

### B. Erratic regime

The connection between the onset of erratic behavior in the forced system and chaotic behavior in the unforced system may be examined by turning off the field at particular times along the trajectory and then allowing the system to evolve in the absence of the forcing term. Shown in Figs. 5(a) and 5(b) are two such examples. The initial conditions for Fig. 5(a) were arrived at during the excitation in the *regular* regime; the quasiperiodic nature of the motion is readily apparent. Quite in contrast is Fig. 5(b); the initial conditions correspond to a point in the erratic regime, and the underlying motion is seen to be typically chaotic. This motion can be examined in another manner. In Fig. 5(c), we follow the crossings of a given trajectory with  $(x=0, p_x > 0)y-p_y$  plane. (The latter is a surface of section for a nonconservative system.) These points, while not forming a closed curve in any way, still congregate about the (positive slope) diagonal—the regions of stability at all energies (cf. Fig. 1). Thus, if three-dimensional surfaces of section were depicted (with energy as the third axis), in the periodic regime the forced trajectory is confined to "tubes of stability." The erratic regime sets in when, at a given energy, the trajectory escapes from a tube of stability and samples the underlying chaos. This motion is thus in accordance with the statistical description for the dissociation process.

In order to study the ensemble of trajectories, we define the average energy function

$$\bar{E}_{av}(t) = \frac{1}{N_s(t)} \sum_{i=1}^{N_s(t)} E_i(t), \quad (5.1)$$

which is shown in Fig. 6. Here  $N_s(t)$  is the number of surviving trajectories at time  $t$ ; overall periodicity of the individual trajectories is retained by the average. The fraction of surviving trajectories  $f_s(t) [= N_s(t)/N_s(0)]$  is depicted in Fig. 7(a). This is seen to be a stepwise decreasing function, with the time separation between the large steps about the same as the period of oscillation of the average energy function in Fig. 6 [i. e., about 5 for 800 time units in Fig. 7(a), compared with five oscillations in 800 time units in Fig. 6]. Further, if the positive slope portions of the energy curve  $E_{av}(t)$  are extrapolated to the dissociation energy, the times of in-

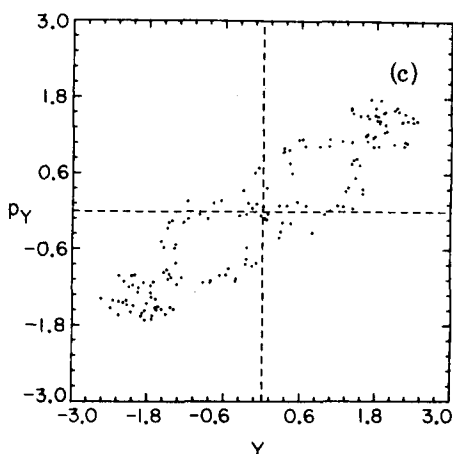
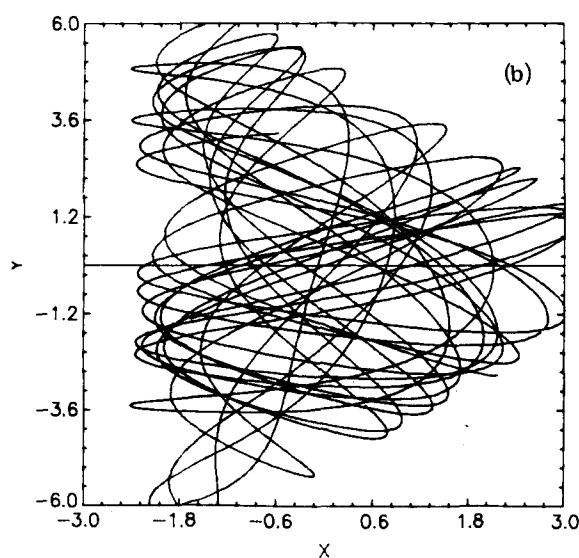
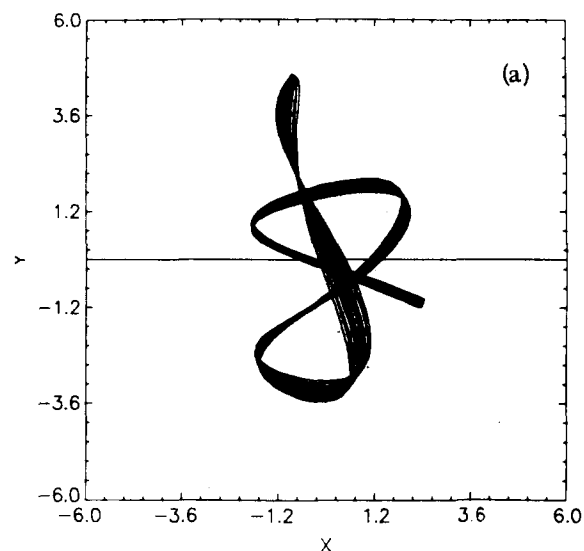


FIG. 5. Trajectories with initial conditions arrived at during the excitation. (a) Initial conditions in the periodic regime. (b) Initial conditions in the erratic regime. (c) Crossings of a typical (forced) trajectory with the  $(x=0, p_x > 0)$   $y-p_y$  plane in the periodic regime.

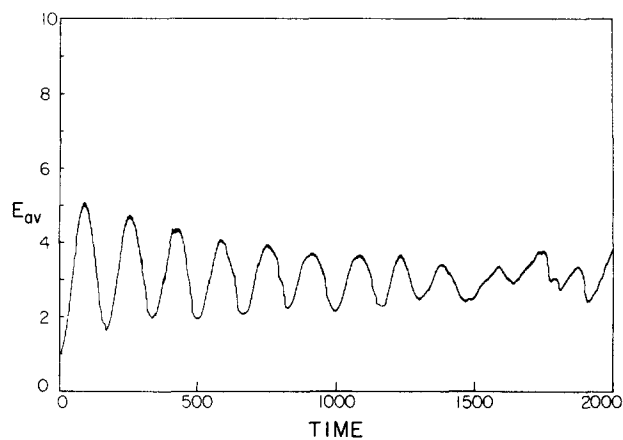


FIG. 6. Average energy behavior for the ensemble of trajectories.

tersection correspond to the *time* of the largest steps in  $f_s(t)$ . On a logarithmic scale,  $f_s(t)$  is very roughly linear (during the first few half-lives), in accord with Eq. (4.18) and has a slope at half life of  $-0.002$ . In applying Eq. (4.18), we estimate  $\zeta = 0.5$ ,  $E_{\max} = 5.0$  (from Fig. 2), and  $\beta = 0.02$  (from Fig. 6). Thus,  $(\beta/\pi)\ln\zeta = -0.004$ . This value agrees to a factor of 2 with the empirical value obtained from Fig. 7(b). It must be emphasized that the model is only a first approximation. The decrease in slope of the  $\ln f_s(t)$  vs  $t$  curve with time in Fig. 7(b), may be due to the residual unreacted systems being "locked" into a regular part of phase space instead of sampling the latter more randomly.

We also studied the system with a weaker driving force  $F = 0.04$ . The maximum energy absorbed is  $\sim 3.0$  units, and at this energy  $\zeta = 1.0$  (cf. Fig. 2). No dis-

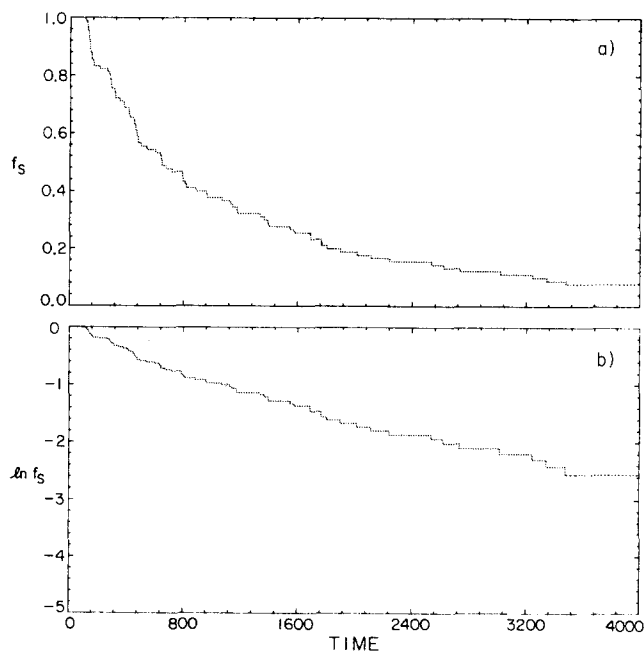


FIG. 7. (a) Fraction of surviving trajectories  $f_s(t)$  as a function of time for  $F = 0.1$ . (b)  $\ln [f_s(t)]$  vs time.

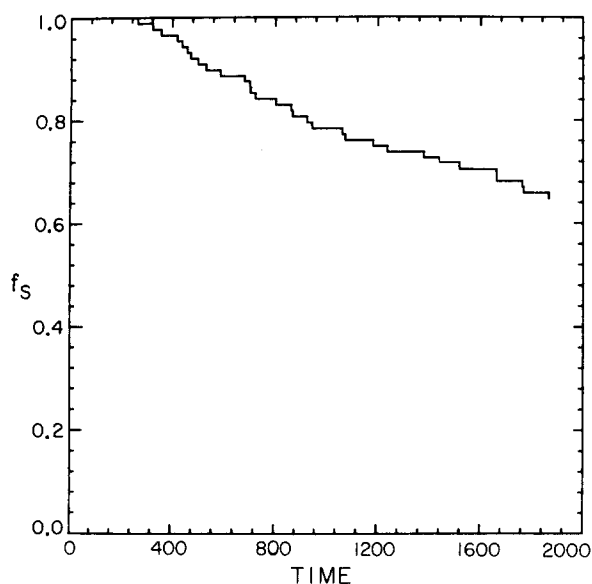


FIG. 8. Same as Fig. 7(a) but with  $F=0.06$ .

sociation was observed in the *entire* sample. With an intermediate power  $F=0.06$ , the energy maximum is  $\sim 4.0$  units when  $\zeta=0.82$ . The observed decay time is consequently longer (see Fig. 8). Here  $(\beta/\pi)\ln\zeta = -0.001$ , which agrees to a factor of 3 with the empirical value of  $-0.0003$ .

## VI. CONCLUSIONS AND SUMMARY

In our study of this problem we have formulated a classical phenomenology of a driven coupled oscillator system. Two essentially different kinds of behavior can be distinguished: The exchange of energy between system and field occurs with a well-defined time scale deriving from several aspects of the motion in the forced and unforced system. Secondly, the energy behavior can become highly erratic, and the latter motion inevitably led to dissociation under the conditions studied. The contrasting periodic and erratic regimes in the forced system have their immediate analog in quasi-periodic and chaotic motion in the autonomous system, respectively.

A time lag is observed in the appearance of dissociation when an ensemble of trajectories is analyzed. This delay is associated with the periodicity of the energy behavior, as the minimum time required to absorb the necessary energy to dissociate. Further, the distribution of lifetimes shows a power-law decay, which is tied into the extent of stability in the motion of the autonomous system. This distribution can be understood semi-quantitatively, and it is demonstrated how the parameters governing the decay rate can be approximately related to the parameters of the system.

Some similar qualitative conclusions were arrived at in Ref. 5(d), where a different two degree of freedom system (harmonic oscillator coupled to a Morse oscillator) with a similar forcing term was studied. For individual trajectories the two regimes of behavior, de-

noted regular and erratic here, were observed, and an entropy-like quantity was used to determine the onset of such erratic behavior. Further, in the regular regime, a minimum intensity was seen to be required to make the chaotic region of phase states accessible, which is consistent with the results presented in Sec. V B.

In larger systems that are more typically "molecular," the analysis will necessarily become more complicated than the present one. The present study shows the need for properly including the role of internal resonances.

In higher-dimensional systems, methods based on spectral characteristics<sup>18</sup> or the Liapunov characteristic number<sup>19</sup> (the mean rate of separation of nearby trajectories) are more suited for measuring the extent of chaos since surfaces of section become considerably more difficult to compute. At this time considerable effort is being devoted in the literature to the prediction of widespread chaos in such systems,<sup>10(b)</sup> and it ultimately may be possible to obtain  $\zeta$  without recourse to numerical experiments.

## ACKNOWLEDGMENT

We are pleased to acknowledge the support of this research by a grant from the National Science Foundation.

- <sup>1</sup>See, for example, N. Bloembergen and E. Yablonovitch, *Phys. Today* **31**, 23 (1978); M. F. Goodman, J. Stone, and E. Thiele, in *Multiple Photon Excitation and Dissociation of Polyatomic Molecules, Topics in Current Physics*, edited by C. D. Cantrell (Springer, New York, 1980).
- <sup>2</sup>See, for example, (a) R. V. Ambartsumian and V. S. Letokhov, *Chemical and Biochemical Applications of Lasers*, edited by C. B. Moore (Academic, New York, 1977), Vol. 2; (b) D. Bomse, R. L. Woodin, and J. Beauchamp, in *Advances in Laser Chemistry*, edited by A. H. Zewail (Springer, New York, 1978); (c) Aa. Sudbø, P. A. Schulz, E. R. Grant, Y. R. Shen, and Y. T. Lee, *J. Chem. Phys.* **70**, 912 (1978); **69**, 2312 (1978); (d) P. A. Hackett, C. Willis, and M. Gauthier, *J. Chem. Phys.* **71**, 2682 (1979); (e) P. Kolodner, C. Winterfield, and E. Yablonovitch, *Opt. Commun.* **20**, 119 (1977).
- <sup>3</sup>(a) M. Quack, *J. Chem. Phys.* **69**, 1282 (1978); (b) N. Bloembergen, C. Cantrell, and D. Larsen, in *Tunable Lasers and Applications*, edited by A. Mooradian, T. Jaeger, and P. Stokseth (Springer, New York, 1976); (c) J. Stone and M. F. Goodman, *Phys. Rev. A* **18**, 2618 (1978); (d) S. Mukamel and J. Jortner, *J. Chem. Phys.* **65**, 5204 (1976); (e) E. R. Grant, P. A. Schulz, Aa. S. Sudbø, Y. R. Shen, and Y. T. Lee, *Phys. Rev. Lett.* **40**, 115 (1978); (f) J. G. Black, E. Yablonovitch, N. Bloembergen, and S. Mukamel, *Phys. Rev. Lett.* **38**, 1131 (1977); (g) E. Yablonovitch, *Opt. Lett.* **1**, 87 (1977); (h) J. Lyman, *J. Chem. Phys.* **67**, 1868 (1977).
- <sup>4</sup>J. T. Lin, *Phys. Lett. A* **70**, 195 (1979); also, W. E. Lamb, paper presented at Conference on Laser Chemistry, Steamboat Springs, Colorado, 1976.
- <sup>5</sup>(a) R. B. Walker and R. Preston, *J. Chem. Phys.* **67**, 2017 (1977); (b) D. Noid, M. L. Koszykowski, R. A. Marcus, and J. D. McDonald, *Chem. Phys. Lett.* **51**, 540 (1977); (c) D. Noid and J. Stine, *Chem. Phys. Lett.* **65**, 153 (1979); (d) K. D. Hansel, *Chem. Phys. Lett.* **57**, 619 (1978).
- <sup>6</sup>P. R. Sethna, *J. Appl. Mech.* **32**, 576 (1965); P. R. Sethna, in *Nonlinear Differential Equations and Nonlinear Mechanics*,

- edited by J. P. LaSalle and S. Lefschetz (Academic, New York, 1963). Equation (4.5) was obtained for the case  $\omega_x = 2\omega_y$ , by assuming  $2\psi_y - \psi_x = 0$  (see Ref. 20). In an exact solution of Eq. (4.5),  $\psi_x$  contains an additional term that is periodic in  $t$  and has a time average of zero. For simplicity, this term was neglected.
- <sup>7</sup>See, for example, H. T. Davis, *Introduction to Nonlinear Differential and Integral Equations* (Dover, New York, 1954); W. J. Cunningham, *Introduction to Nonlinear Analysis* (McGraw-Hill, New York, 1958); A. H. Nayfeh and D. T. Mook, *Nonlinear Oscillations* (Wiley, New York, 1979).
- <sup>8</sup>(a) V. I. Arnold, *Mathematical Methods of Classical Mechanics* (Springer, New York, 1978); (b) J. Ford, in *Fundamental Problems in Statistical Mechanics*, edited by E. D. G. Cohen (Elsevier, New York, 1975); (c) See Appendix 8 in Ref. 8(a).
- <sup>9</sup>(a) M. Henon and C. Heiles, *Astron. J.* **69**, 73 (1964); (b) D. W. Noid and R. A. Marcus, *J. Chem. Phys.* **62**, 2119 (1975); D. W. Noid, M. L. Koszykowski, and R. A. Marcus, *J. Chem. Phys.* **71**, 2864 (1979), and references therein.
- <sup>10</sup>(a) See P. Brumer, *Adv. Chem. Phys.* (in press) for a review; (b) See M. Tabor, *Adv. Chem. Phys.* (in press) for a review.
- <sup>11</sup>(a) S. Chapman, B. Garrett, and W. Miller, *J. Chem. Phys.* **64**, 502 (1976); (b) K. Sorbie and N. Handy, *Mol. Phys.* **32**, 1327 (1976); (c) G. Schatz and M. D. Moser, *Chem. Phys.* **36**, 239 (1978).
- <sup>12</sup>The quantum energy levels were determined using standard matrix diagonalization programs.
- <sup>13</sup>Integrations of Eq. (3.2) were performed on a VAX 11/780 computer using Fortran programs.
- <sup>14</sup>N. N. Bogoliubov and Y. A. Mitropolsky, *Asymptotic Methods in the Theory of Nonlinear Oscillations* (Hindustan, New Delhi, 1961).
- <sup>15</sup>(a) G. Hori, *Publ. Astron. Soc. Jpn.* **18**, 287 (1966); **23**, 567 (1971); (b) A. Deprit, *Celest. Mech.* **1**, 12 (1969); (c) A. A. Kamel, *Celest. Mech.* **3**, 90 (1970).
- <sup>16</sup>(a) G. Hori, *Publ. Astron. Soc. Jpn.* **19**, 229 (1967); (b) G. E. O. Giacaglia, *Perturbation Methods in Nonlinear Systems* (Springer, New York, 1972); (c) The autonomous system has a near 2:1 resonance, and so the near-resonant algorithm in (a) was used. The  $\eta$  term, which contributes relatively little to  $\tilde{\omega}_y$ , was neglected, and to obtain Eq. (4.15) the  $q_1$  in Eq. (49) of Ref. 16(a) was set equal to  $\pi$  for simplicity. (See Ref. 20.)
- <sup>17</sup>In a preliminary report [R. Ramaswamy and R. A. Marcus, in *Classical, Semiclassical, and Quantum Mechanical Problems in Mathematics, Chemistry, and Physics*, edited by K. Gustavson and W. P. Reinhardt (Plenum, New York, in press)] an agreement was reported for a single numerical and perturbation calculated amplitude and period in the quasi-periodic regime, but was fortuitous.
- <sup>18</sup>R. A. Marcus, D. W. Noid, and M. L. Koszykowski, in *Advances in Laser Chemistry*, edited by A. Zewail (Springer, New York, 1978); D. W. Noid, M. L. Koszykowski, and R. A. Marcus, *J. Chem. Phys.* **67**, 404 (1977); G. E. Powell and I. Percival, *J. Phys. A* **12**, 2053 (1979).
- <sup>19</sup>G. Benettin, L. Galgani, and J. M. Strelcyn, *Phys. Rev. A* **14**, 2338 (1976).
- <sup>20</sup>Simple stability analysis [W. J. Cunningham, *Introduction to Nonlinear Analysis* (McGraw-Hill, New York, 1958)] at the equilibrium points for the resonant angle  $\theta$  and its conjugate momentum [which are  $q_1$  and  $p$  in Ref. 16(a)] and are the variables  $\frac{1}{2}\omega_x a_x^2$  and  $(\omega_x - 2\omega_y)t + \psi_x - 2\psi_y$ , in the KBM-type analysis) shows that the equilibrium points at which  $\theta = 0$  or  $\theta = \pi$  are of neutral stability. In both of the perturbation treatments in Sec. IV,  $\theta$  was replaced for simplicity by one of its equilibrium values. The value chosen for the Lie transform treatment ( $\theta = \pi$ ) was that which gave the smallest imaginary eigenvalue. In the KBM case the eigenvalues were complex conjugates for 0 and  $\pi$  and the value used ( $\theta = 0$ ) was an *ad hoc* one which gave best numerical results.